sciendo

Mathematical Modelling in Civil Engineering
Vol. 17-No. 2 : 1-12-2022
Doi: 10.2478/mcee-2022-0006

MAPPING OF THE LIQUEFACTION INDEX, CASE STUDY

Souad BENAHCHILIF – PhD, RISk Assesment & Management Laboratory (RISAM), University of Tlemcen**,** Algeria/ e-mail: nesouad@yahoo.fr

Salah Eddine BOUGUERBA – Dr RISk Assesment & Management Laboratory (RISAM), University of Tlemcen, Tlemcen, 1300, Algeria, email: swilah32@gmail.com

Abstract: The present work uses a number of empirical models from geotechnical earthquake engineering (CPT-based liquefaction models) in combination with some geostatistics tools to assess the soil liquefaction potential over an extended area at the Airport of Algiers (Algeria), by the kriging approach. The SIG software program along with variograms and the kriging method were all applied together for the purpose of modeling the variation of the liquefaction potential (PL) against liquefaction in the region under study. This approach allowed determining the missing data in that region. This geostatistical method helped to draw maps at different soil depths. The results obtained revealed that the models developed were potentially capable of accurately estimating the needed data. This study made it possible to determine a number of parametric quantities that support the empirical correlation between the liquefaction potential index and liquefaction. The results show that the higher the standard deviation, the greater the uncertainty.

Keywords: Kriging; CPT; Site investigations; liquefaction index PL, SIG

1. Introduction

Soil liquefaction is a seismic ground failure process that takes place in loose, saturated granular sediments, mainly in sand and silty sand. This mechanism turned out to be the primary cause for the damage of soil structures, lifeline facilities, and building foundations in previous seisms. Indeed, today soil liquefaction should be viewed as a real concern as it clearly poses serious threats to the integrity of structures and facilities in the case of any possible future earthquakes in Algeria and around the world as well.

Soil liquefaction potential at the Airport of Algiers may be evaluated through the use of a number of geotechnical data such as the type of soil, CPT value, depth of water table, mean grain size of soil particles and soil specific weight. These geotechnical data were gathered from subsoil investigation reports (geotechnical borehole logs), as indicated in Figure 1.

It is worth specifying that the borehole data for the study area were collected at different depths, ranging from 10 m to 20 m below ground surface.

In order to determine the liquefaction potential in the areas where the borehole data are not available, a special statistical analysis was carried out by means of the Geographic Information System (GIS).Geostatistics is closely linked to interpolation procedures, but covers much more than simple interpolation issues in order to prepare a continuous map.

It is worth indicating that interpolation is about evaluating a variable at an indefinite position based on values collected in surrounding areas. A Kriging method of interpolation was employed in the present study for the purpose of interpolating the liquefaction potential.

It is important to note that the geostatistical methods were initially used for mineral reserve calculations in the pioneering study of Krige, (Wang 1999) Afterwards, the theory was reformulated in a very short form by the remarkable contributions of George Matheron. Subsequently, a novel scientific discipline, namely geostatistics, came into existence by uniting Krige's concepts and Matheron's theory of regionalized variables [1].

This geostatistical interpolation technique takes into account both the distance and the degree of variation between given data points when the data to be estimated are in unknown areas.

Note that kriging supposes that the distance or direction between sample points corresponds to a special correlation that can be employed in describing and elucidating the variation at the surface [1].

This is a technique that allows making optimal, unbiased estimates of regionalized variables at locations not previously sampled, using the essential properties of the semivariogram as well as the initial set of data values.

Moreover, it aims to minimize the error variance and to fix the mean of the prediction errors to zero in order to prevent any overestimations or underestimations.

The present study aims at mapping the factor of safety against liquefaction (FS) through the use of geostatistical methods. The results were mapped using the Geographic Information System (GIS) software.

Furthermore, the results found were validated by comparing the real or absolute values with the estimated ones in two boreholes. These data were then used for liquefaction analysis.

2. Investigation area

As a first step, it was decided to conduct an expertise of the basement and foundations, in the course of the construction of a new terminal and a freight station at Algiers International Airport. The site under study, namely the Airport of Algiers, is located about 20 km south-east of the city of Algiers, in the great coastal Mitidja plain which lies between the mountains of the Tellian Atlas and the Mediterranean sea. The location of the penetrometer tests is given in Figure 1. [2]

The behavior of the water table under the site study ground exhibited significant variations of up to 5 m, depending on the season. It was therefore advisable to consider that the water table was flush.

Note that for each penetrometric curve, the values of the peak resistance qc and lateral friction force fs were recorded every 0.15 m to a depth of up to 20 m, depending on the rejection of the test as a result of the penetrometer entering in contact with rocky soil. The boring locations as well as the boundaries of the area under consideration are mentioned in Figure 1.

The liquefaction potential index was calculated for each CPT profile for an earthquake scenario with Mw = 6.8 and having a peak horizontal ground acceleration amax = 0.3 g. The CPT positions were defined by the Universal Transverse Mercator (UTM 31 Zone 31N) coordinate system as well as the raw data of the results of the CPT test on the site in consideration and shown in the table 1 for a depth of 0.5m.

Table 1

Penetrometric Data for z=0.5 m

Borehole	Coordinates		qc (Kpa)	fs(Kpa)	Borehole	Coordinates		qc (Kpa)	fs(Kpa)
	Easting (m)	Northing (m)				Easting (m)	Northing (m)		
BH1	519039.1	4062223	43	3,37	BH32	4040744	24.11	19	1.35
BH2	519247.8	4061957	15,3	1,15	BH33	4061421	16.97	35	2.45
BH3	519471.7	4061669	12.2	0.8	BH34	4060166	12.66	22	1.94
BH4	519697.4	4061414	16.1	1.01	BH35	4060353	26.85	18	1.24
BH5	519931.9	4061204	17.4	0.91	BH36	4060620	26.54	39.5	1.87
BH6	519925.8	4060761	15.3	1.07	BH37	4060475	21.12	42	0.58
BH7	519655.4	4061015	26.5	1.25	BH38	4061284	23.9	17.4	0.83
BH8	519438.6	4061314	13.5	1.03	BH39	4061850	30.48	30.6	2.08
BH9	519187.1	4061546	24.9	1.74	BH40	4061971	32.72	58.3	3.43
BH10	518939.2	4061757	20.4	1.16	BH41	4059634	27.74	27.5	2.13
BH11	518750.8	4062111	32	2.28	BH42	4061729	29.61	24.7	1.65
BH12	519674.6	4060860	19.5	2.39	BH43	4059841	13.44	21	1.66
BH13	519369.7	4060970	20.8	1.82	BH44	4060130	12.45	22	1.42
BH14	519124.5	4061169	22.5	1.5	BH45	4059942	23.93	25.5	1.25
BH15	518443.2	4061889	28.4	3.4	BH46	4061656	19.64	19.6	0.36
BH16	519199.3	4060493	25.5	1.4	BH47	4061644	6.18	31.9	1.6
BH17	518900	4060902	24	1.4	BH48	4058514	0.93	16.5	0.56
BH18	518591	4061257	23.8	1.38	BH49	4058736	0 .00	17.1	0.93
BH19	518848	4060181	23.75	0.88	BH50	4058958	0.00	27.6	1.39
BH20	518474.9	4060857	13.3	0.53	BH51	4059125	0.21	23.8	1.44
BH21	518374.6	4060557	18.4	1.74	BH52	4058892	0.00	24.3	1.44
BH22	518288	4060102	17	1.26	BH53	4058648	3.24	20.3	1.03
BH23	518125.3	4059736	71.5	2.35	BH54	4058348	0.00	27.7	1.17
BH24	517678.6	4059724	33.8	1.43	BH55	4058870	1.83	25	2.13
BH25	517901.1	4060124	20	1.25	BH56	4058681	5.21	17.5	1.05
BH26	518152.4	4060413	25.3	1.25	BH57	4058493	1.61	15.2	0.72
BH27	518130.8	4060901	18.5	1.03	BH58	405854	6.00	89.5	3.2
BH28	517660.5	4060689	18.8	1	BH59	4059143	3.29	17	0.94
BH29	517854.7	4060945	15.4	1.22	BH60	4059410	4.85	21.4	1.29
BH30	517444.4	4059335	15.5	0.8	BH61	4059687	11.92	29	1.92
BH31	517097.9	4061032	20	1.5	BH62	4059487.6	11.66	25.7	1.83

3. Liquefaction potential of soil using data obtained from the Cone Penetration Test

The approach initially suggested by Robertson and Wride (1998), and afterwards updated by Robertson (2009) for the assessment of the liquefaction potential of sandy soils employing data provided by the Cone Penetration Test (CPT), is adopted in the present study [3].

It is interesting to mention that the form given below is selected for the Cyclic Stress Ratio [7]:

$$CSR_{7.5} = \frac{\tau_{av}}{\sigma'_v} = 0.65 \cdot \frac{a_{\max}}{g} \cdot \frac{\sigma_v}{\sigma'_v} \cdot \frac{r_d}{MSF} \frac{1}{K\sigma} \tag{1}$$

Where amax is the peak horizontal acceleration generated by the earthquake at the ground level, g is the gravitational acceleration, σv and σ'v are the total and effective vertical overburden stresses, respectively, and rd the depth-dependent shear-stress reduction coefficient.

Also, MSF is the magnitude scaling factor, and Kσ the overburden correction factor for the cyclic stress ratio (CSR).Furthermore, the form given below is adopted for the shear-stress reduction factor rd [9] .

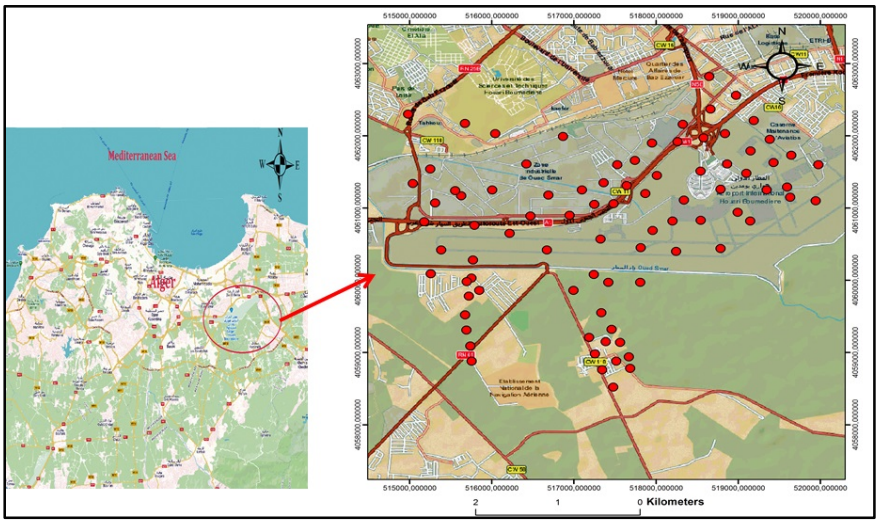

Fig.1 - Investigation area borehole locations

$$r_d = \frac{1 - 0.4113 \times Z^{0.5} + 0.04052 \times Z + 0.001753 \times Z^{1.5}}{1 - .4177 \times Z^{0.5} + 0.05729 \times Z - 0.006205 \times Z^{1.5} + 0.001210 \times Z^{2}} \tag{2}$$

As for the magnitude scaling factor (MSF), the lower-bound equation that was proposed [9] is used:

$$MSF = \left(\frac{M_w}{7.5} \right)^{-2.56} \tag{3}$$

Similarly, the cyclic resistance ratio (CRR) is evaluated according to the method developed by Robertson and Wride (1998) and updated by Robertson (2009), as expressed below: [3]

$$CRR = \begin{cases} 0.833 \left(\frac{q_{c1N,cs}}{100} \right) + 0.05 & for\ q_{c1N,cs} < 50 \\ 93 \left(\frac{q_{c1N,cs}}{100} \right)^3 + 0.08 & for\ 50 \le q_{c1N,cs} < 160 \end{cases} \tag{4}$$

Where the clean-sand equivalent normalized cone tip resistance (qc1N)cs is defined as:

$$(q_{c1N}) = K_c \times q_{c1N} \tag{5}$$

Here Kc is the conversion factor that is expressed as:

$$\begin{cases} K_c = 1 & for\ I_c \leq 1.64 \\ K_c = -0.403I_c^4 + 5.58I_c^3 + 33.75I_c - 17.88 & for\ I_c > 1.64 \end{cases} \quad (6)$$

On the other hand, the soil behavior type (SBT) index Ic was defined as: [10]

$$I_c = [(3.47 - logQ)^2 + (1.22 + logF)^2]^{0.5} \quad (7)$$

Note also that the normalized tip resistance Q and the normalized friction ratio F are stated as:

$$Q = \left[\frac{(q_c - \sigma_{v0})}{P_a}\right](\frac{P_a}{\sigma'_{v0}})^n \quad (8)$$

$$F = \left[\frac{f_s}{(q_c - \sigma_{v0})}\right] \times 100\% \quad (9)$$

Taking into account the two quantities CSR and CRR, the factor of safety against liquefaction may therefore be expressed as [11]:

$$FS = \frac{CRR_{7.5}}{CSR} \cdot MSF \cdot K_\sigma \quad (10)$$

4. Determination of the liquefaction potential index

The first step consists of determining the safety factor (FS), and the second one is to find the liquefaction potential index (LPI), which is a measure of the total risk of liquefaction of soil to a depth of 20 m. The liquefaction potential index is defined as follows: [7]

$$LPI = \int_0^{20} F(z)\, w(z)\, dz \quad (11)$$

Furthermore, Tatsuoka classify a site, according to the importance of the soil liquefaction phenomenon, into five categories: Very low for LPI = 0, Low for 0 < LPI ≤ 2, Moderate for 2 < LPI ≤ 5, High for 5 < LPI ≤ 15, and Very high for LPI > 15.

5. The Geostatictical Kriging Interpolation Method

Geostatistics is a branch of statistics applied to problems in geology and hydrology. It is increasingly employed in mapping regionalized variables. Kriging is a geostatistical approach that offers the advantage of preserving the spatial continuity of the parameters for a possible mapping. [6]

It is worth indicating that in the geostatistical kriging algorithm, the weighting rule and, consequently, the resulting map can straightforwardly be determined based on the spatial behavior of the characteristics of the element to be examined.The preliminary step to using kriging is the variographic analysis which is carried out for the purpose of assessing the function of the spatial continuity of a regionalized variable [9].

The variogram γ(h) can be described as the magnitude of dependence between attributes at two different locations:

$$2\gamma(h) = Var[Z(u + h) - Z(u)] \quad (12)$$

Note that 2γ(h) is the value of the variogram corresponding to a separation distance h, Z(u) is the value of the random variable q at position u, Z(u+h) is the value of the previous random variable at a distance h from Z(u), and Var [] is the variance operator. [3].

Three model parameters, namely Nugget, Range, and Sill, were obtained after fitting the semivariogram model; these parameters were employed in describing the nature of spatial variability. The parameter Range represents an estimate of the maximum distances over which the measured parameter Z is spatially correlated.

Note that as h increases, the semivariogram.value rises to a specific degree, but remains unchanged for values greater than the parameter known as the Sill. The semivariogram value is 0 at zero separation distance; this is called the nugget effect which represents the unexplained or random variance that is mainly attributed to errors occurring during sampling and measurements.

In this study, the semivariogram models were applied for the purpose of estimating the spatial distribution of safety factors against liquefaction through ordinary kriging.

It is important to recall that a kriged estimate is defined as a linear estimator of the variable Z at location u in space, where the value of Z is unknown; this is achieved by means of kriging interpolation techniques.

The kriged estimate depends on various features of the spatial correlation structure, i.e. variogram, but does not change from one situation to another. This estimate may be evaluated on the basis of the expression below: [1]

$$Z^*(u) = \sum_{i=1}^{n} \lambda_i Z(u_i) \qquad (13)$$

Here Z(ui) is a value of Z at position ui; it is provided either from field data at that position or from antecedently simulated nodes

Z (ui) is a weight that is assigned to field data at position ui; it is dependent on the characteristics of the spatial correlation structure.

6. Results and discussion

In this study, the kriging method was applied using the SIG software. Various variograms were developed with data collected at depth. The ordinary kriging method was employed to prepare the index liquefaction, maps after fitting the appropriate theoretical mathematical models to experimental variograms.

The statistical distribution of the Liquefaction Potential Index (LPI) is illustrated by the histogram in Figure (2). The Kurtosis coefficient (1.79) is greater than 0, which implies that the distribution is more flattened than a normal distribution. The Skewness coefficient (0.47) indicates that this distribution is not symmetrical; it is an asymmetric distribution, with a spread towards the low values. Therefore, a logarithmic transformation could certainly help to make the distribution of the data more symmetrical. However, this transformation is not recommended by several authors. (Table 2)

Henry's line shows that the distribution of the soil liquefaction potential index LPI does not follow a Gaussian law.(Figure 3).

If the property of normality has the advantage of completely defining the distribution by its mean and its standard deviation, it is not an obligatory condition in linear geostatistics. This makes no particular assumption about the distribution of values. (Figure 3), [5].

Table 2

Basic Statistics for Liquefaction Potential Index

Count	62	Skewness	0.47
Min	0	Kurtosis	1.79
Max	32.718	1-St Quartille	1.6
Mean	11.456	Median	8.67
Std Dev	10.45	3- quartille	21.116

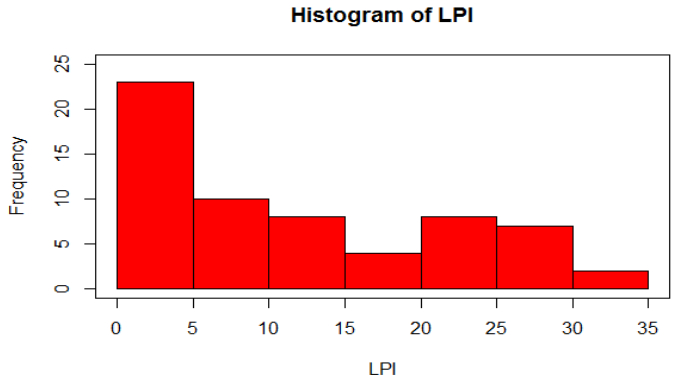

Fig.2 - Histogramme de l'indice du potentiel de liquéfaction (LPI)

The evolution of the soil liquefaction potential (LPI) as a function of x (east-west direction) and y (north-south direction) to detect the presence of a spatial drift is shown in the figure 4, if it exists, it should translate graphically into an increase or decrease in the scatter plot.

These figure show that no relationship of the LPI values with x and y is clearly evident. The behavior of the soil liquefaction potential index (LPI) along the principal directions of space gives an idea of the validity of a stationarity hypothesis.

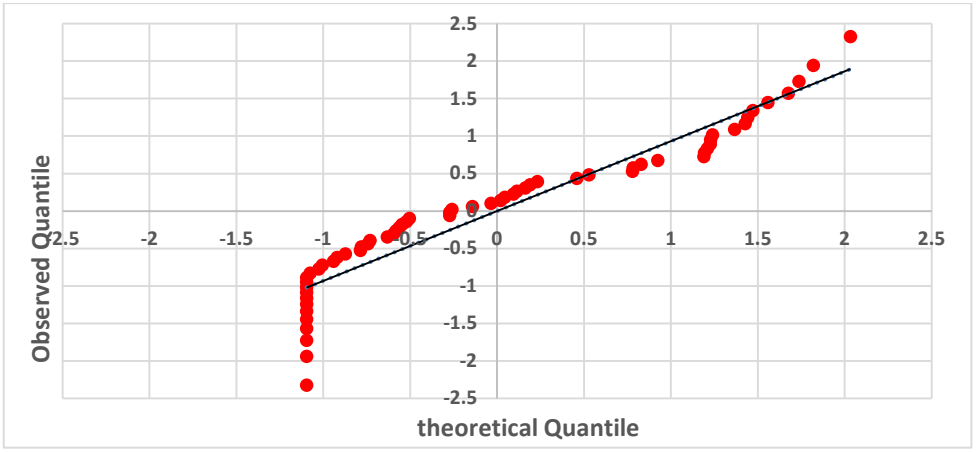

Fig.3 - Quantile-Quantile Plots of Soil Liquefaction Potential (LPI)

7. The variographic cloud

To study the variability and the numerical stability of the experimental variogram, it is useful to visualize the "variographic cloud", that is to say the cloud of points used to calculate the experimental variograms.

We observe that the dispersion of the cloud tends to increase with the distance h, this means that we are all the more likely to find pairs of dissimilar data when their separation is large. (Figure 5).

It is also possible to examine the variographic cloud from different directions.

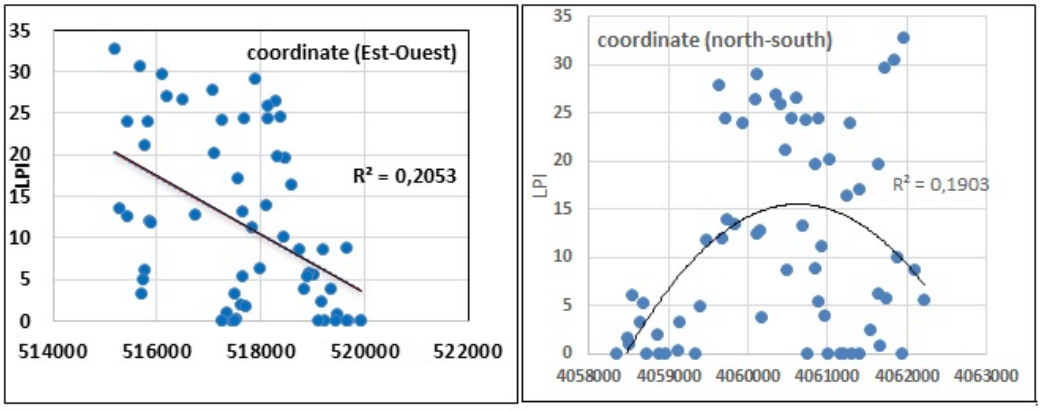

Fig. 4 - The soil liquefaction potential index (LPI), east-west and orth-south coordinate,

It is possible to see if the values are influenced in a preferred direction. This is called anisotropy. Different parameters are involved: the width of the band (bandwidth), the tolerance angle and the direction angle.

8. Omnidirectionnel variogramme

The experimental variogram makes it possible to characterize the spatial continuity of the regionalized variable studied (LPI).

A simplifying assumption is to assume that the regionalization is isotropic and to calculate an omnidirectional variogram. On Figure 5 we find the experimental omnidirectional variogram, calculated for distance multiples of a step of 300 meters

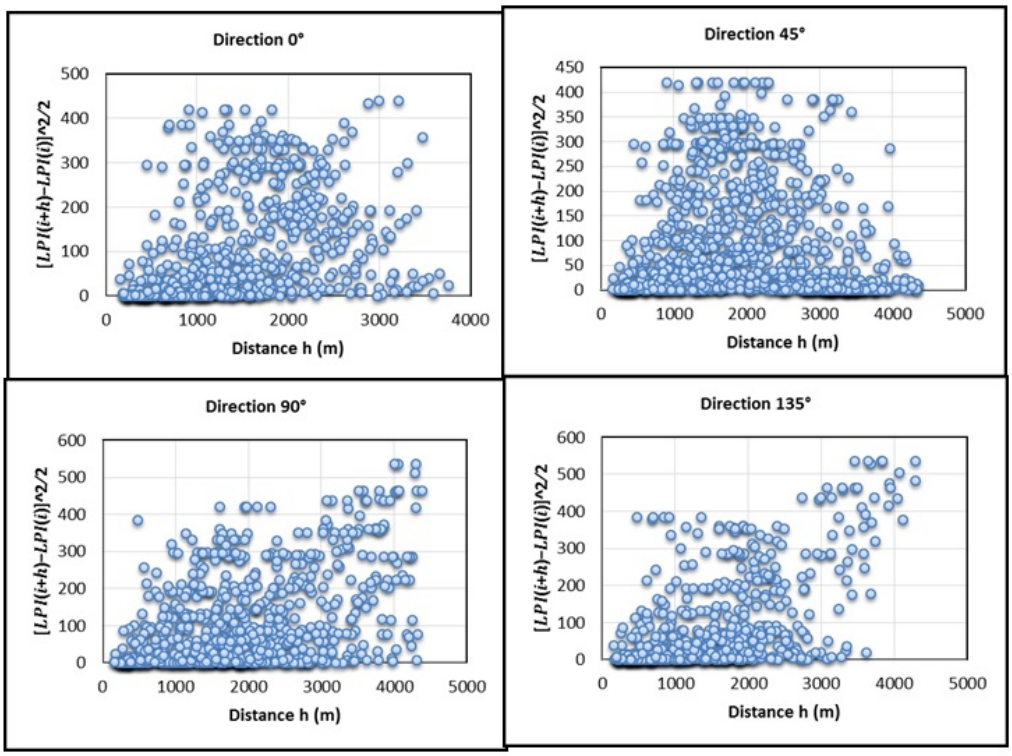

Fig. 5 - Soil Liquefaction Potential Index (LPI) Variographic Could

The numbers of data pairs involved in the calculation of the experimental points are indicated in the figure 6; they are all greater than 31, which indicates that these experimental points can be considered reliable.

The experimental variogram stabilizes around a plateau equal to 120 from h=1800m. This level is close to the statistical variance of the data. We can deduce that the regionalized variable (LPI) is a

realization of a stationary random function of order 2. At a very short distance, the experimental variogram seems to tend towards a zero value, which indicates a great regularity of the regionalized variable (LPI) which translates into the absence of the nugget effect.

The experimental variograms according to the directions 0°, 45°, 90° and 135° with respect to the north-south direction were calculated for multiple distances given by the following table 2.

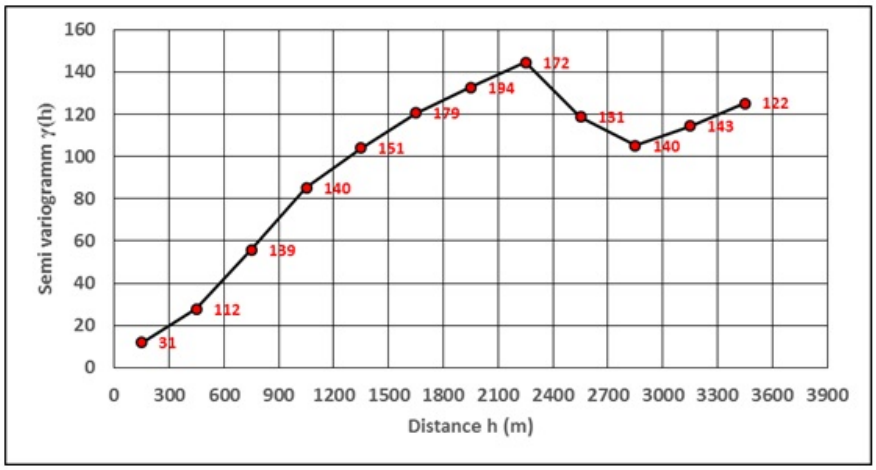

Fig. 6 - Experimental omnidirectional variogram of the soil liquefaction potential (LPI)

Table 2

Main parameters relevant to the experimental variograms

	Nugget Effect (Co)	Range (m)	the calculation step	Number of steps	Tolerance angle	Bandwidth (lag)
0°	0	1350	300	12	45	3
45°	0	1300	200	12	45	3
90°	0	2600	260	12	45	3
135°	0	1875	250	12	45	3

To model the experimental variogram, a theoretical model was adjusted to the experimental model, and then the parameters determining the model was adjusted (the range, the still and the nugget effect). (Figure 7).

The theoretical model which is close to experimental variogram after trying other theoretical models available in "geostatistical analysis" of the GIS is that of spherical which defines by the following formula:

$$\gamma(h) = \begin{cases} c_0 + c\left(\frac{3h}{2a} - \frac{h^3}{2a^3}\right) & for\ 0 < h < a \\ c_0 + c & for\ h > a \end{cases} \quad (14)$$

The theoretical adjustment model is chosen according to the highest coefficient of determination R2 and the lowest sum of squares of deviations (RSS). (Table 3)

Considering the results presented by table 3, the spherical model gives the best description of the experimental semi-variogram, with a high R2 of 0.943, a very low RSS of 1728 and a small nugget effect of 0. The ratio C/(C0+C) is 1, which indicates a strong spatial correlation up to a range (a) of 1800 m, beyond which there is no influence between the soundings.

Table 3

Parameters of the semi-variograms adjusted for the index of the potential of soil liquefaction (LPI)

Model type	Nugget C0	Partial Sill C+C0	Range a (m)	C/C+C0	RSS	R2
Spherical	0	120	1800	1	1728	0.943
Exponential	0	135	1060	1	2633	0.885
Linear	38	146	3440	0.735	7272	0.629
Gaussian	5	125	1200	0.96	2205	0.900

The range of the variogram (a) is a measure of the limit of spatial continuity of soil properties and it provides valuable information about the neighborhood in which the measurement points influence the estimation of LPI values in unmeasured locations.

A model is considered valid if the correlation coefficient between the estimated values and the measured values must be as close as possible to 1, the histogram of the standardized errors is tightened and centered on 0 and the correlation cloud the standardized errors and the estimated values is close to the first bisector.

9. Kriging mapping

Ordinary kriging mapping of the soil liquefaction index (LPI) over the entire study site was carried out.

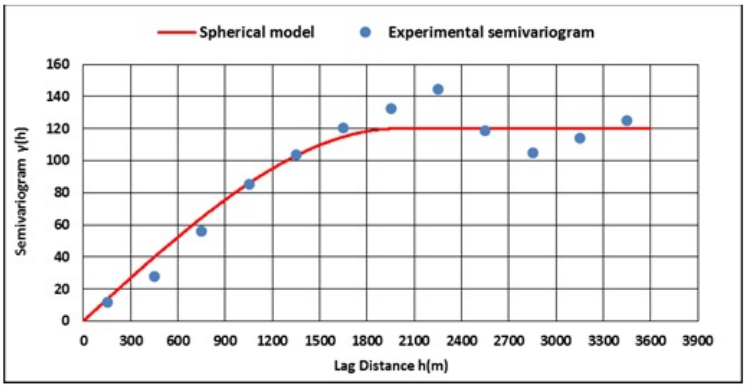

Fig.7 - Experimental omnidirectional variogram and isotropic spherical model of liquefaction

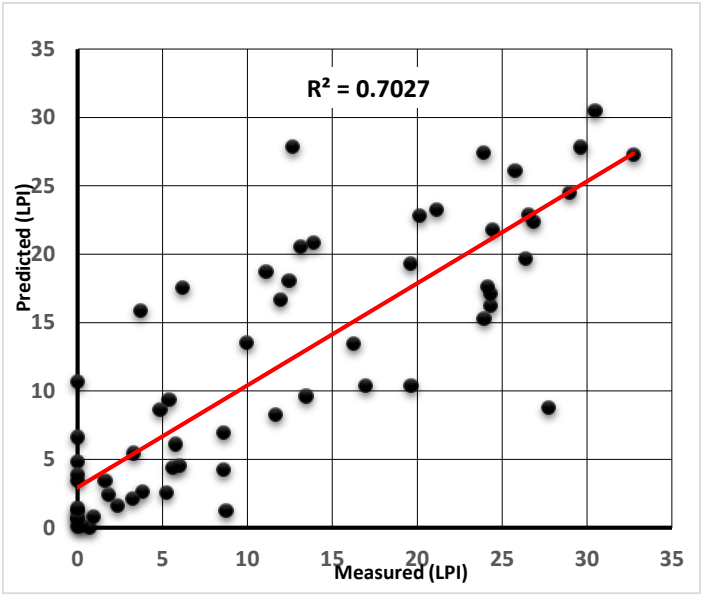

Fig. 8 - Correlation cloud between true and estimated values (isotropic model)

The maps of the results of interpolation by ordinary kriging as well as that of the corresponding standard deviation of kriging have been determined.

The map resulting from ordinary kriging interpolation and the corresponding kriging standard deviation presented in Figure 9 and Figure 10.

We can therefore visualize the regions where the estimate is precise and the regions where

the imprecise estimate where it would be appropriate to measure.

The kriging standard deviation does not depend on the measured values of LPI, it depends only on the model of variogram and measurement point distributions.

Spatial variations in kriging standard deviation indicate loss of precision when moving away from the measurement points.

They provide information on areas where the sampling is sufficiently dense (low standard deviation good precision) and on those where it is too far apart (large standard deviation, mediocre precision). The standard deviation of kriging quantifies the possible dispersion of the true, but unknown, value around the estimated value.

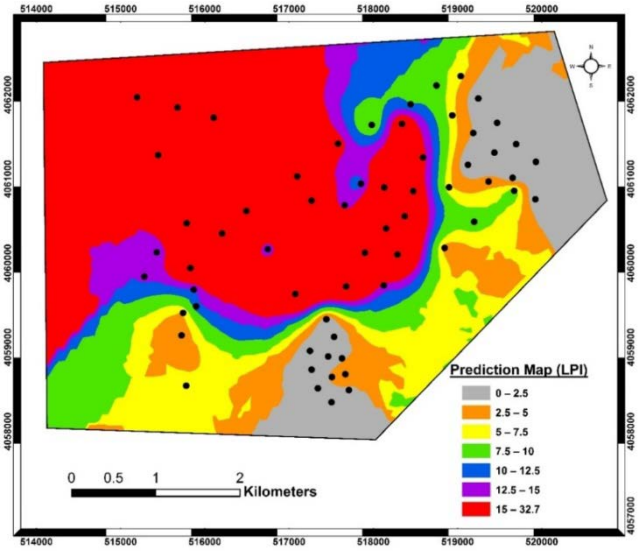

Fig. 9 - Map of potential liquefaction risks predicted by ordinary kriging for earthquake magnitude of 6.8 and maximum ground acceleration of 0.3g (isotropic analysis)

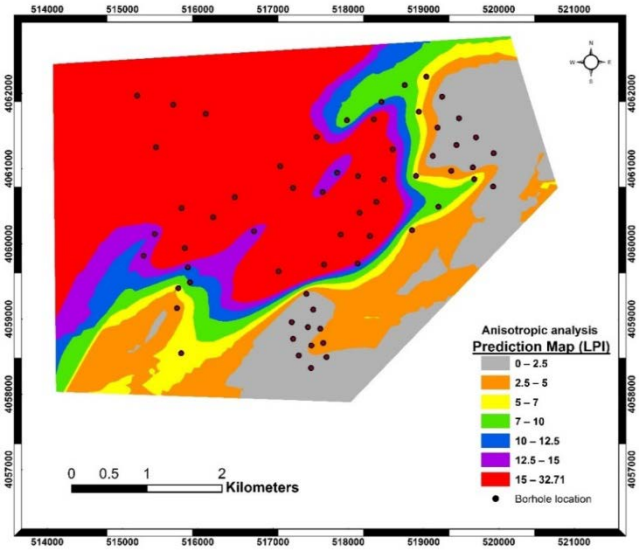

Fig 10 - Map of potential liquefaction hazards predicted by ordinary kriging for an earthquake magnitude of 6.8 and peak ground acceleration of 0.3g (isotropic analysis)

10. Conclusions

The city of Algiers (Algeria) is a highly seismic area, and therefore, soil liquefaction poses a major concern for structures resting on sandy soil. A campaign of 62 static penetration tests or cone penetrometer tests (CPT) was carried out on a site located in the commune of Dar El Beïda in Algiers. The soil Liquefaction Potential Index (LPI) values were assessed, for each borehole, based on the simplified procedure of Seed and Idriss. On the other hand, the geographic information system and geostatistical analysis were used to quantify the risk of soil liquefaction at the studied site.

The coupling of GIS Geographic Information System techniques and geostatistical analysis allows us to spatially model the risk of soil liquefaction over the entire studied site of Algiers Airport, by digital maps of spatial distribution estimates potential soil liquefaction index (LPI).

Another important tool of geostatistical analysis is Kriging standard deviation maps of predicted values (LPI), these maps identify areas of uncertainty. The results show that the higher the standard deviation, the greater the uncertainty.

The presence of a large area that is susceptible to this liquefied; especially in the northwest of the study area was shown by the results.

The kriging standard deviation does not depend on the measured values of LPI, it depends only on the variogram model and the distributions of the measurement points. The results show that there is a proportional relationship between the risk of liquefaction and the increase or decrease in seismic acceleration.

References

[1] Bacconnet, C. (1991). *Géostatistique et géotechnique, application à la reconnaissance des sols*. Thése Université Blaise pascal,Clermont ferrand II.

[2] Benahchilif, S. (2016). *Mise en place d'une approche fiabiliste pour l'estimation du potentiel de liquefaction, thèse de Doctorat*, Université Abou Bakr belkaid,Tlemcen.

[3] Benahchilif et al. (2016). *Assessing of liquefaction in Boumerde (Algeria) using reliabilityanalysis.*

[4] Juan Camilo Gomez et al. (2019). *Assessment of earthquake-induced- risk of soil liquefaction using CPT-based methods: application to the case study of Cavezzo municipality (Italy).* Vol. 21, EGU2019-11247-2, 2019.

[5] Selim- Altun et al. (2013). *Geostatistical interpolation for modelling SPT data in northern Izmir* Sa¯dhana¯ Vol. 38, Part 6, December 2013, pp. 1451–1468._c Indian Academy of Sciences.

[6] Iwasaki,T., Tatsuoka,F., Tokida,K.,Yasuda,S. (1978). A practical method for assessing soil liquefaction potential based on case studies at various sites in Japan. In: Proceedings of the 2nd international conference on Microzonation, 885–896.

[7] Idriss, I.M., and Boulanger, R.W. (2006). *Semi-empirical procedures for evaluating liquefaction potential during earthquakes.* J. Soil Dynamics and Earthquake Eng. 26, 115–30. Rama Mohan Pokhrel et al, 2012 Geostatistical analysis for spatial evaluation of liquefaction potential in Saitama City International Association of Lowland Technology (IALT), ISSN 1344-9656, Vol. 14, No. 1, 45-51, June 2012

[8] Ross W. Boulanger et al. (2014). *CPT and SPT based liquefaction riggering procedures.* Report No. UCD/CGM-14/01, April 2014.

[9] Idriss, I.M., and Boulanger, R.W. (2006). *Semi-empirical procedures for evaluating liquefaction potential during earthquakes.* J. Soil Dynamics and Earthquake Eng. 26, 115–30

[10] Salah Eddine Bouguerba et al. (2021). *Geostatistical analysis of spatial variability of the liquefaction potential in the area of Algiers Airport (Algeria)*, Studia Geotechnica et Mechanica. 43(2): 155–168

[11] Youd, T. L., Idriss, I. M., Andrus, R. D., Arango, I., Castro, G., Christian, J. T., Dobry, R., Finn, W. D. L., Harder, L. F., Hynes, M. E., Ishihara, K., Koester, J. P., Liao, S. S. C., Marcuson, W. F., Martin, G. R., Mitchell, J. K., Moriwaki, Y., Power, M. S., Robertson, P. K., Seed, R. B., and Stokoe, K. H. (2001). *Liquefaction resistance of soils: summary report from the 1996 NCEER and 1998 NCEER/NSF workshops on evaluation of liquefaction resistance of soils*. J. Geotechnical and Geoenvironmental Eng., ASCE 127(10), 817–33.